

Supporting Information

Atomic Engineering in Covalent Organic Frameworks for High-Performance Proton Conduction

Lina Zong[†], Shanshan Tao[‡], Xiaoyi Xu[†], Yaoqian Feng[†], Fuxiang Wen[†], Ning Huang^{†,}*

[†]State Key Laboratory of Silicon and Advanced Semiconductor Materials, Department of Polymer Science and Engineering, Zhejiang University, Hangzhou 310058, China

[‡]Department of Chemistry, Faculty of Science, National University of Singapore, 3 Science Drive 3, Singapore 117543, Singapore

Table of Contents

Section A. Methods and Materials-----	S2
Section B. Characterization-----	S14
Section C. Supporting Tables-----	S24
Section D. Supporting References-----	S25

Section A. Methods and Materials

Methods.

Proton nuclear magnetic resonance (^1H NMR and ^{13}C NMR) spectra were measured on Bruker Avance III 400 (400 MHz) NMR spectrometer. Electrospray ionization time-of-flight massspectrometry (ESI-TOF MS) was obtained on a 6200 series TOF/6500 series Q-TOF B.09.00 high resolution mass spectrometer. Fourier-transform infrared (FTIR) spectra was performed on a Nicolet 6700 using KBr pellets from 4000 to 400 cm^{-1} . The data was treated with OPUS spectroscopy software. Solid-state ^{13}C cross-polarization/magic-angle-spinning (CP/MAS) NMR spectra were recorded by a Bruker Avance-500 NMR spectrometer. The spinning rate and acquisition time were 10 kHz and 0.0378 s respectively. The SEM images were obtained from a Hitachi model S-4800 field-emission scanning electron microscope (FE-SEM). instrument with an accelerating voltage of 3.0 kV. High-resolution transmission electron microscopy (HR-TEM) was carried out on a JEM 2100F high-resolution microscopy. Cryo-transmission electron microscopy (cryo-TEM) was carried out on a Titan Krios microscopy. All the COF samples were prepared through drop super-sonicated acetone suspensions of samples onto copper grids. The thermal stability of these materials was evaluated from the thermogravimetric analysis (TGA) using the Mettler Toledo TGA instrument under pure nitrogen. The samples were heated to 200 $^{\circ}\text{C}$ for 30 min to remove the trapped solvents. After return to room temperature, the samples were heated to 800 $^{\circ}\text{C}$ at a rate of 10 $^{\circ}\text{C min}^{-1}$. Powder X-ray diffraction (PXRD) was performed using Rigaku fabricated Miniflex-600c, and the POP powder was detected from 2.0 $^{\circ}$ to 30.0 $^{\circ}$ with a step width of 0.01 $^{\circ}$. The scanning speed of the measurement was 10 $^{\circ} \text{min}^{-1}$. Nitrogen sorption isotherms and water isotherms were measured by BELSORP-max II Brunauer-Emmett-Teller (BET) theory and Cylinder non-local density functional theory (NLDFT) were used to evaluate the surface area and

pore volume respectively of all materials. OCA-20 contact goniometer was applied to measure the static and dynamic water contact angles of the samples using a 10 μ l water drop.

Preparation of PA@COFs

Neat phosphoric acid (calculated values, **Table S1**) was dissolved in anhydrous tetrahydrofuran (4 mL). The solution was then added to the COFs (100 mg) in a vial (10ml) which had been pre-treated under vacuum at 120°C overnight. After stirring at room temperature for 3 h, the mixture was heated at 70°C under vacuum to remove tetrahydrofuran over a period of 6 h. Subsequently, the vial was placed in an oven at 120°C for 12 h. The resulting powder was collected, to yield PA@COFs quantitatively.

Pellet preparation

The pellets of PA@COFs were prepared through a standardized procedure: initially, the PA@COFs samples were ground into a homogeneous powder using a mortar and pestle under a dry atmosphere. Subsequently, the resulting powder was loaded into a standard 10 mm die and compressed at 100 kN for 120 minutes to form pellets. To ensure proper electrical contact, both surfaces of the pellets were coated with conductive silver paste (Sigma-Aldrich) to create electrodes. The conductivity measurements were conducted using a HIOKI IM3570 impedance analyzer equipped with a two-probe electrochemical cell. The measurements were performed across a frequency range of 4 Hz to 5 MHz, with an input voltage amplitude of 100 mV. Throughout the measurements, the cell was maintained under a protective dry N₂ atmosphere. To ensure reproducibility, each conductivity value was determined from at least three independently prepared sample batches.

Impedance spectroscopy

The pellets were coated with conductive silver paste (Sigma) to form electrodes on both sides. Proton conductivity was measured using a HIKIO IM3570 impedance analyzer with a two-probe cell over the frequency from 4Hz to 5Hz and with an input voltage of 100 mV. The cell was protected by dry N₂ during testing. Each conductivity value was verified through at least three sets of samples.

Materials.

The following chemicals were purchased from Energy Chemical Corporation: ethanol, mesitylene, benzyl alcohol, glacial acetic acid (AcOH), ethyl acetate (EA), 1,2-N,N-dimethylformamide (DMF), tetrahydrofuran (THF), acetone, anhydrous hexane, nitrobenzene, dioxane, dichloromethane (CH₂Cl₂), petroleum ether (PE), hydrochloric acid (HCl), trifluoroacetic acid (CF₃COOH), sodium hydroxide (NaOH), sodium bicarbonate (NaHCO₃), cesium carbonate (Cs₂CO₃), and potassium carbonate (K₂CO₃). Additionally, 4,4,5,5-tetramethyl-1,3,2-dioxaborolane-2-yl pyrene, (4-boc-aminophenyl)boronic acid, bis(pinacolato)diboron (B₂pin₂), 4,4'-di-tert-butyl-2,2'-bipyridine, tetrakis(triphenylphosphine)palladium(0) [Pd(PPh₃)₄], [Ir(μ-OMe)cod]₂, and 4-formylphenylboronic acid pinacol cyclic ester were acquired from Adamas Reagent Corporation. Bromine and hydrogen peroxide (H₂O₂, 30 wt%) were obtained from Shanghai Lingfeng Chemical Reagent Co., Ltd. All solvents and starting chemicals were used without further purification.

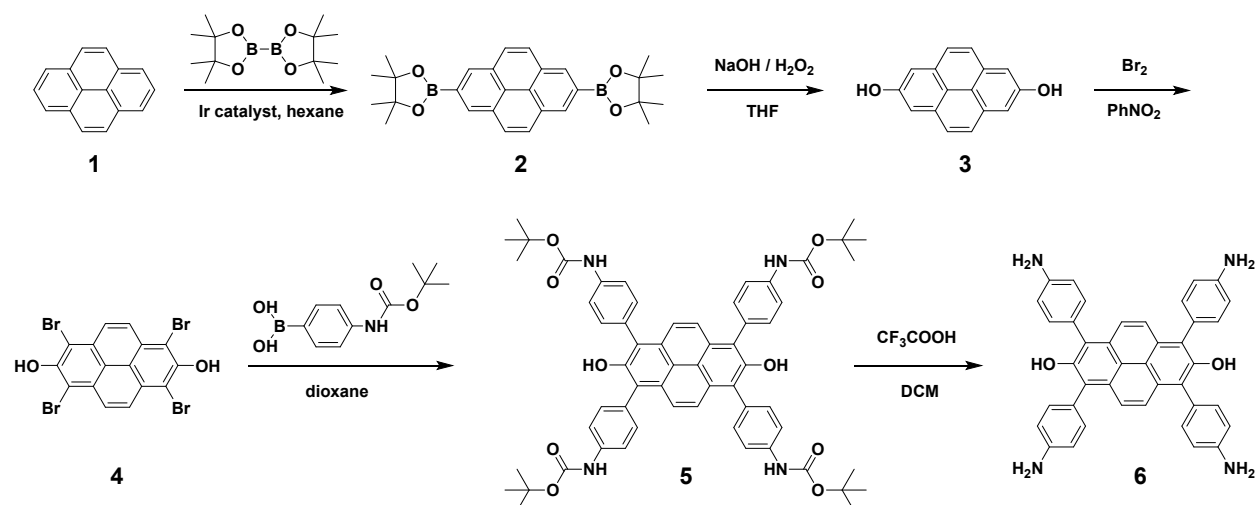


Figure S1. Synthetic routine of DHPy(NH₂)₄

2,7-Bis(4,4,5,5-tetramethyl-1,3,2-dioxaborolan-2-yl) pyrene (2): Pyrene (5 g, 24.7 mmol) and B₂pin₂(12 g, 48 mmol) were weighed into a 250 mL two-necked flask. A condenser was installed onto the flask. After that, [$\text{Ir}(\mu\text{-Ome})\text{cod}$]₂(0.26 g, 0.25 mmol), 4,4'-di-tert-butyl-2,2'-bipyridine (dtbpy, 0.25 g, 0.05 mmol) were quickly weighed into the flask. Anhydrous hexane (60 mL) were added to dissolve all reagents and then vacuumed/flushed with nitrogen three times. The reaction mixture was stirred at 85 °C for 48h. After cool to the room temperature, the reaction mixture was passed through a 5 cm silica plug (eluent: CH₂Cl₂) and the solvent was removed under reduced pressure. The crude product was subjected to flash column chromatography: hexane / CH₂Cl₂=1:1. The desired product was obtained as a white powder (4.6 g, 40 %). ¹HNMR (400 MHz, DMSO-D₆) δ (ppm) 8.61 (s, 4H, Ar-H), 8.08 (s, 4H, Ar-H), 1.46 (s, 24 H, -CH₃).

2,7-Dihydroxypyrene (3): Compound 2 (4.6 g, 10.13 mmol) and NaOH (2.43 g, 60.77 mmol) were dissolved in THF (400 mL). After stirring at room temperature for 10min, an aqueous solution of H₂O₂ (7.5ml, 30 wt %) and H₂O (15ml) was added to this mixture. After stirring at room temperature for 6 h, 200ml H₂O was added and the solution was acidified to pH 1-2 by using

1M HCl. The precipitated product was collected by filtering and washed with water. After that, the product was further vacuum dried at 50 °C. The desired product was obtained as a taupe brown powder (2.27 g, 95 %). ¹H NMR (400 MHz, DMSO-D₆) δ (ppm) 9.89 (s, 2H, OH), 7.94 (s, 4H, Ar-H), 7.60 (s, 4H, Ar-H).

1,3,6,8-Tetrabromo-2,7-dihydroxypyrene(4): Under a nitrogen atmosphere, a mixture of bromine (1.75 mL, 34.15 mmol) with 10 mL of nitrobenzene was added dropwise to a solution of compound **3** (1 g, 4.27 mmol) in nitrobenzene (60 mL). The mixture was vigorously stirred at 120 °C for 24 h. After being cooled to room temperature to yield a brown precipitate, the mixture was filtered with hexane (200 mL) under reduced pressure to afford compound **4** as a light-green solid (2 g, 85%), which was insoluble in common organic solvents, such as chloroform and DMSO, but slightly dissolve in ethanol. The product was not further purified and used as such for the Suzuki coupling reactions directly. The solid was characterized by HRMS: HRMS (ESI) m/z [M – H]⁻ Calcd. for C₁₆H₃Br₄O₂ 544.7029, found 544.7025.

1,3,6,8-Tetrakis(4-aminophenyl)-2,7-dihydroxypyrene (6): Compound **4** (1.5 g, 2.73 mmol), (4-boc-aminophenyl) boronic acid (4.18 g, 21.82 mmol), and CsCO₃ (5.3 g, 16.38 mmol) were dissolved in a mixture of dioxane (10 mL), and H₂O (2 mL). The solution was degassed and purged with nitrogen three times. Under a nitrogen atmosphere, Pd (PPh₃)₄ (630 mg, 0.546 mmol) was added, and the mixture was vigorously stirred at 100 °C for 48 h. After being cooled to room temperature, the solution was diluted with CH₂Cl₂ (100 mL) and filtered through a plug of Silica gel powder. The solvent was then removed in vacuo. and the resulting crude material was purified via column chromatography (EA/PE=1:1) to yield compound **5** (1.31 g, 80%). Compound **5** (1.31g, 1.31mmol) was dissolved in CH₂Cl₂ (10 mL). The solution was acidified with CF₃COOH (4 mL, 52 mmol), and the resulting solution was allowed to stir at room temperature for 1 h. The solution

was adjusted to PH 7-8 by using saturated NaHCO₃ solution. The precipitated product was collected by filtering and washed with water. The desired product was obtained as a light green powder (0.6 g, 76%). ¹H NMR (400 MHz, DMSO-D₆) δ (ppm) 7.48(s, 4H, Ar-H), 7.31 (s, 2H, OH), 7.02 (d, 8H, Ar-H), 6.67 (d, 8H, Ar-H), 5.15(s, 8H, NH₂). ¹³C NMR (400 MHz, DMSO-*d*₆): 149.35, 148.35, 132.34, 128.81, 125.77, 124.95, 123.29, 120.15, 114.36. HRMS (ESI) Calcd. For C₄₀H₃₀N₄O₂ [M]⁺: 599.2442. Found: 599.2439.

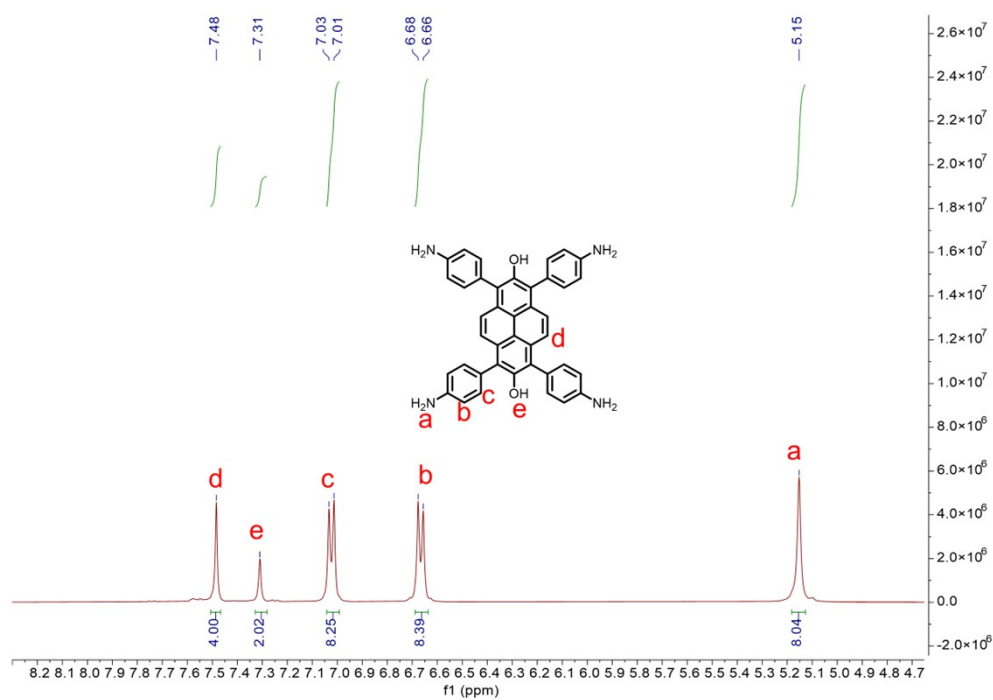


Figure S2. ¹H NMR of DHPy(NH₂)₄

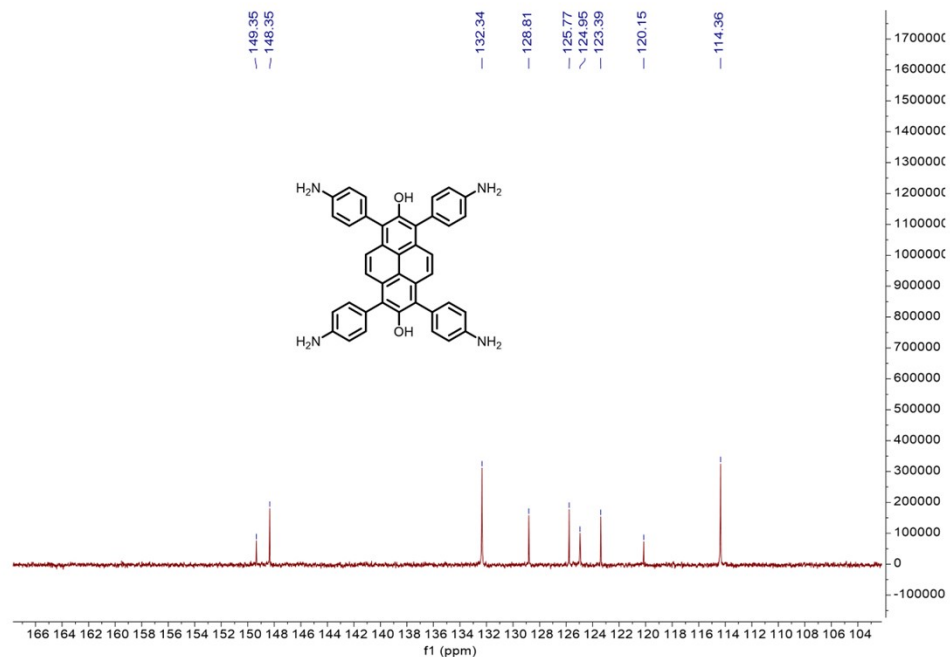


Figure S3. ^{13}C NMR of $\text{DHPy}(\text{NH}_2)_4$

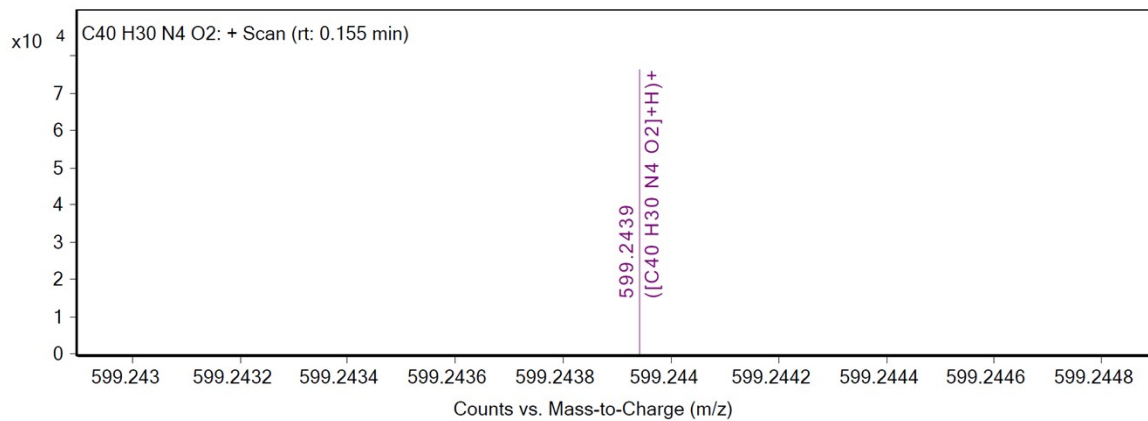


Figure S4. HRMS (ESI) of $\text{DHPy}(\text{NH}_2)_4$

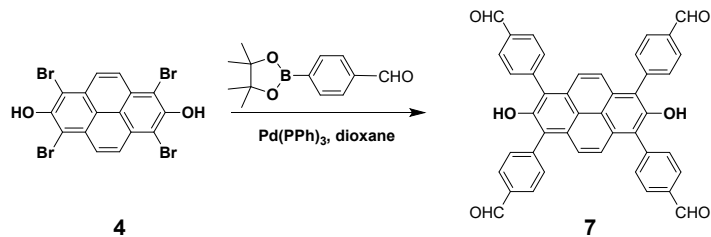


Figure S5. Synthetic route of $\text{DHPy}(\text{CHO})_4$

1,3,6,8-Tetrakis(4-formylphenyl)-2,7-hydroxypyrene (7): Compound 4 (1.5 g, 2.73 mmol), 4-formylphenylboronic acid pinacol cyclic ester (5.17 g, 21.82 mmol), and CsCO₃ (5.3 g, 16.38 mmol) were dissolved in a mixture of dioxane (10 mL), and H₂O (2 mL). The solution was degassed and purged with nitrogen three times. Under a nitrogen atmosphere, Pd (PPh₃)₄ (630 mg, 0.546 mmol) was added, and the mixture was vigorously stirred at 100 °C for 48 h. After being cooled to room temperature, 20mL water was added to the solution and 1M HCl was used to acidify the solution to PH=7. The precipitate was collected after filtering and washed with water and methanol. The desired product was obtained as yellow powder (860 mg, 50%). ¹H NMR (400 MHz, DMSO-D₆) δ (ppm) 10.15(s, 4H, CHO), 8.61(s, 2H, OH), 8.11(d, 8H, Ar-H), 7.73(d, 8H, Ar-H), 7.55(s,4H, Ar-H). ¹³C NMR (400 MHz, DMSO-*d*₆):193.54, 143.58, 135.66, 132.83, 129.95, 128.90, 126.16, 125.47. HRMS (ESI) Calcd. For C₄₄H₂₆O₆ [M]⁻: 649.1657. Found: 649.1656.

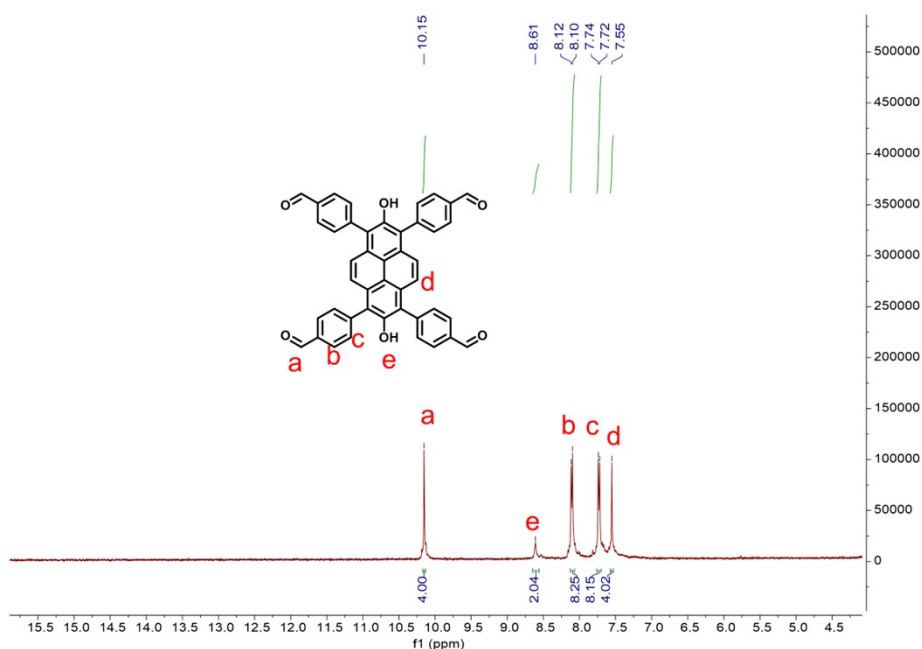


Figure S6. ^1H NMR of $\text{DHPy}(\text{CHO})_4$

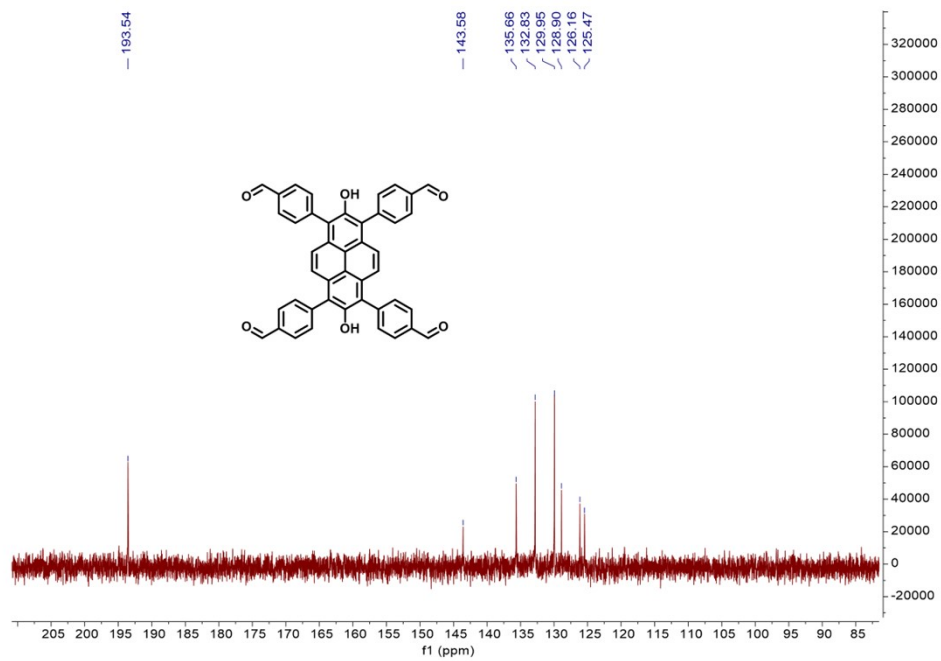


Figure S7. ^{13}C NMR of $\text{DHPy}(\text{CHO})_4$

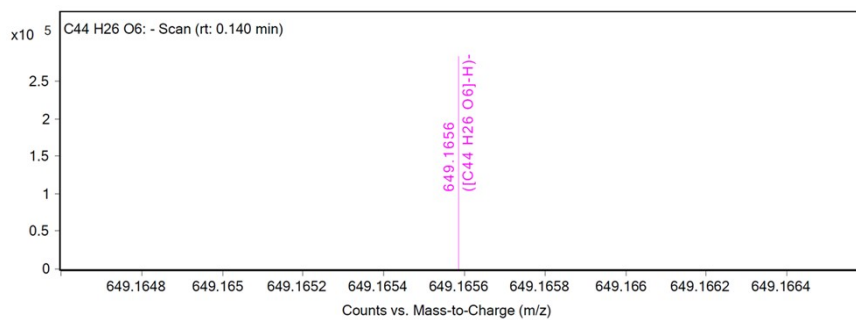


Figure S8. HRMS (ESI) of $\text{DHPy}(\text{CHO})_4$

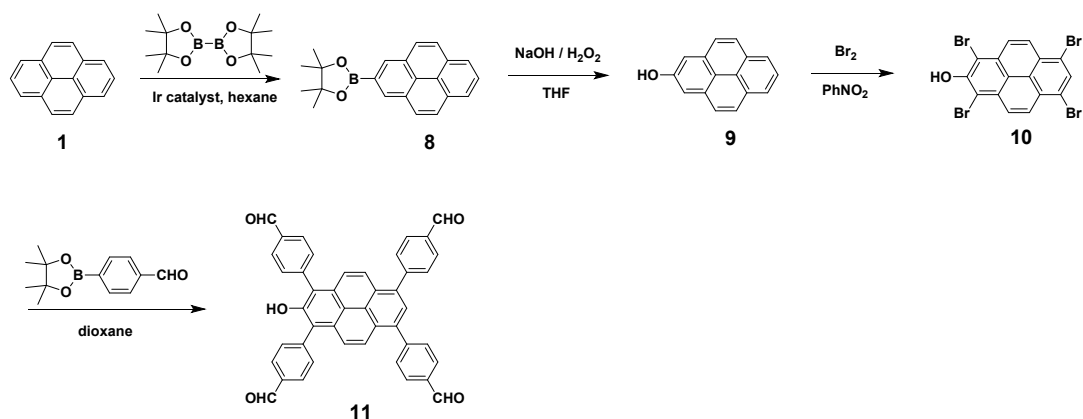


Figure S9. Synthetic route of SHPy(CHO)₄

2-[Bpin]pyrene (8): Under a nitrogen atmosphere pyrene (3 g, 14.8 mmol) were weighed into a 250 mL three-necked flask with 80 ml degassed hexane. A condenser was installed onto the flask. After that, [$\text{Ir}(\mu\text{-Ome})\text{cod}\}_2$] (102 mg, 150 μmol), 4,4'-di-tert-butyl-2,2'-bipyridine (dtbpy, 78 mg, 300 μmol) were quickly weighed into the flask. A solution of *bis*(pinacolato)diboron (596 mg, 2.35 mmol) in degassed hexane (100 ml) was dropped to the suspension during 6 h at 80 °C. The reaction mixture was stirred for 48 h at 80 °C. After cool to the room temperature, the reaction mixture was passed through a 5 cm silica plug (eluent: CH_2Cl_2) and the solvent was removed under reduced pressure. The crude product was subjected to flash column chromatography: hexane / $\text{CH}_2\text{Cl}_2=1:1$. The desired product was obtained as a white powder (1.4 g, 28.8%). ¹H NMR (400 MHz, DMSO- D_6) ¹H NMR (400 MHz, CDCl_3) δ (ppm) 8.63 (s, 2H, Ar-H), 8.16 (d, 2H, Ar-H), 8.05(q, 4H, Ar-H), 8.00(t, 1H, Ar-OH), 1.46 (s, 12 H, - CH_3).

2-Hydroxypyrene (9): Compound **8** (1.4 g, 4.27 mmol) and NaOH (785 mg, 19.62 mmol) were dissolved in THF (200 mL). After stirring at room temperature for 10min, an aqueous solution of H_2O_2 (1.5 ml, 30 wt %) and H_2O (2.5 ml) was added to this mixture. After stirring at room temperature for 6 h, 200 ml H_2O was added and the solution was acidified to pH 1-2 by using 1M HCl. The precipitated product was collected by filtering and washed with water. After that, the

product was further vacuum dried at 50 °C. The desired product was obtained as a taupe brown powder (800 mg, 86 %). ¹H NMR (400 MHz, DMSO-D6) δ (ppm) 9.67 (s, 1H, OH), 7.79 (d, 2H, Ar-H), 7.65 (q, 4H, Ar-H), 7.53 (t, 3H, Ar-H).

1,3,6,8-Tetrabromo-2-hydroxypyrene (10): Under a nitrogen atmosphere, a mixture of bromine (1.5 mL, 29.32 mmol) with 10 mL of nitrobenzene was added dropwise to a solution of Py-OH (800 mg, 3.67 mmol) in nitrobenzene (50 mL). The mixture was vigorously stirred at 120 °C for 24 h. After being cooled to room temperature to yield a brown precipitate, the mixture was filtered with hexane (200 mL) under reduced pressure to afford compound 10 as a light-green solid (1.7 g, 87%), which was insoluble in common organic solvents, such as chloroform and DMSO, but slightly dissolve in ethanol. The product was not further purified and used as such for the Suzuki coupling reactions directly. The solid was characterized by HRMS: HRMS (ESI) m/z [M – H]⁻ Calcd. for C₁₆H₃Br₄O 528.7079, found 528.7077.

1,3,6,8-Tetrakis(4-formylphenyl)-2-hydroxypyrene (11): Compound 10 (500 mg, 0.97 mmol), 4-aminophenylboronic acid pinacol ester (1.12 g, 4.83 mmol), and K₂CO₃ (600 mg, 4.34 mmol) were dissolved in a mixture of dioxane (10 mL), and H₂O (2 mL). The solution was degassed and purged with nitrogen three times. Under a nitrogen atmosphere, Pd (PPh₃)₄ (100 mg, 0.087 mmol) was added, and the mixture was vigorously stirred at 100 °C for 48 h. After being cooled to room temperature, 20mL water was added to the solution and 1M HCl was used to acidify the solution to PH=7. The precipitate was collected after filtering and washed with water and methanol. The desired product was obtained as yellow powder (300 mg, 50%). ¹H NMR (400 MHz, DMSO-*d*₆) δ (ppm) 10.16(d, 4H, CHO), 8.81(s, H, OH), 8.12(q, 8H, Ar-H), 8.06(s, 2H, Ar-H), 7.99(s, 1H, Ar-H), 7.94(d, 4H, Ar-H), 7.77(d, 4H, Ar-H). ¹³C NMR (400 MHz, DMSO-*d*₆): 193.48, 150.09, 146.34, 143.02, 135.53, 135.93, 135.69, 132.84, 131.73, 130.22, 130.17,

126.94, 125.89, 125.69, 125.39. HRMS (ESI) Calcd. For $C_{44}H_{26}O_6$ $[M]^-$: 633.1707. Found: 633.1707.

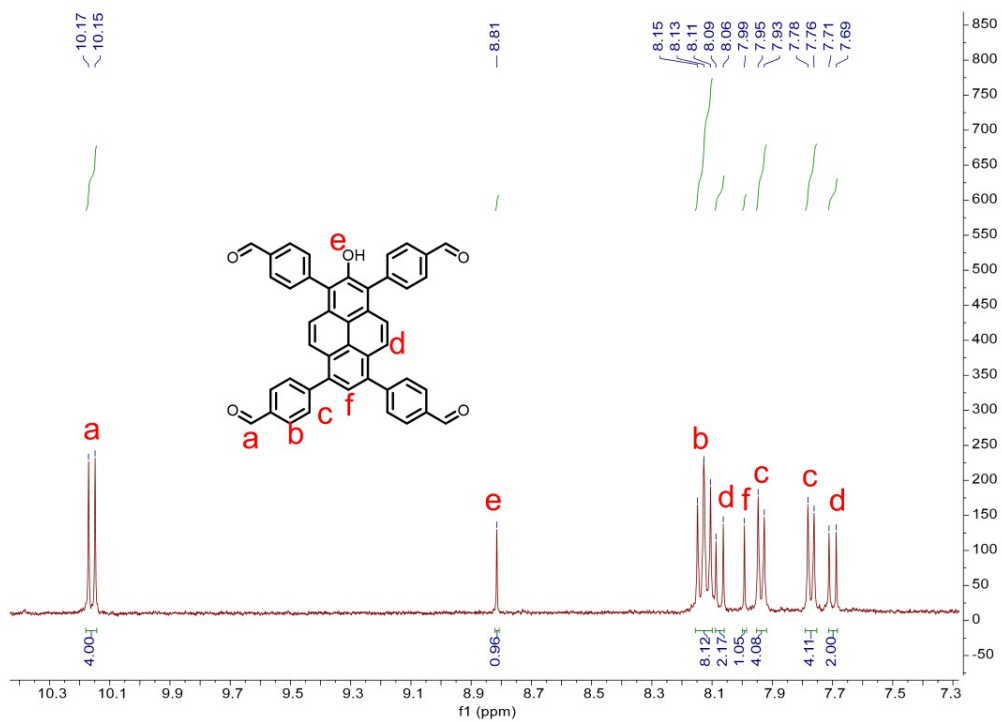


Figure S10. 1H NMR of SHPy(CHO) $_4$

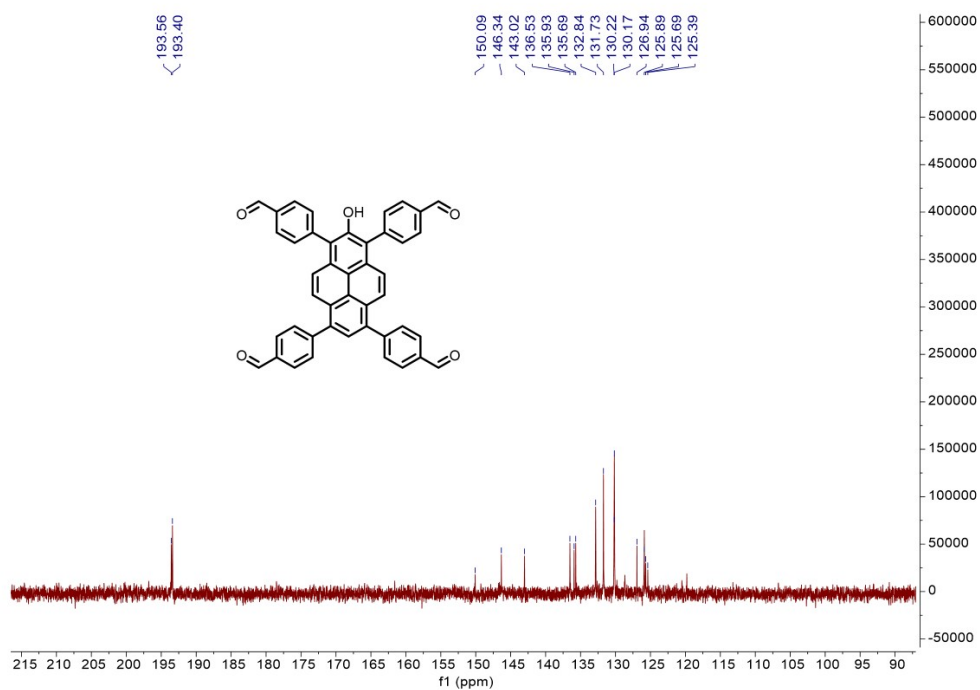


Figure S11. ^{13}C NMR of $\text{SHPy}(\text{CHO})_4$

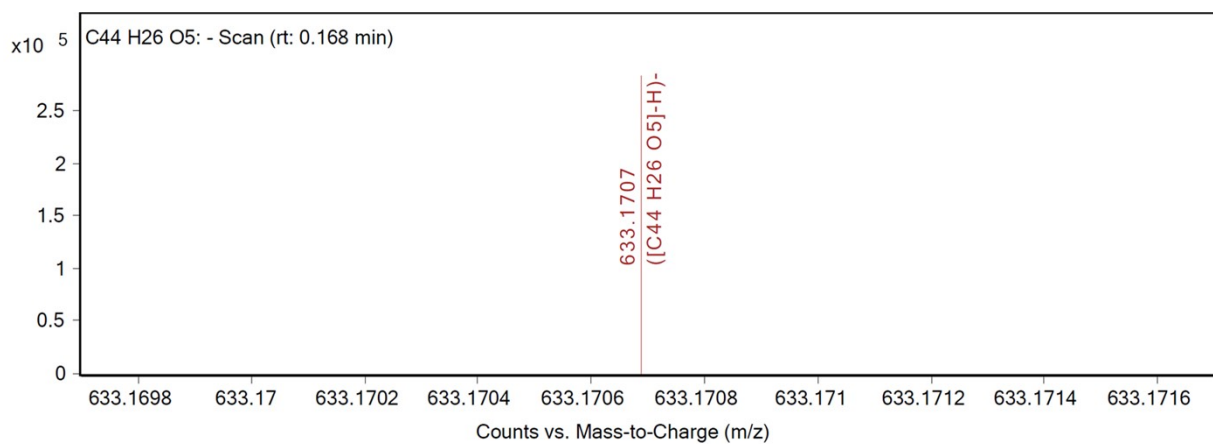


Figure S12. HR-MS (ESI) of $\text{SHPy}(\text{CHO})_4$

Section B. Characterization

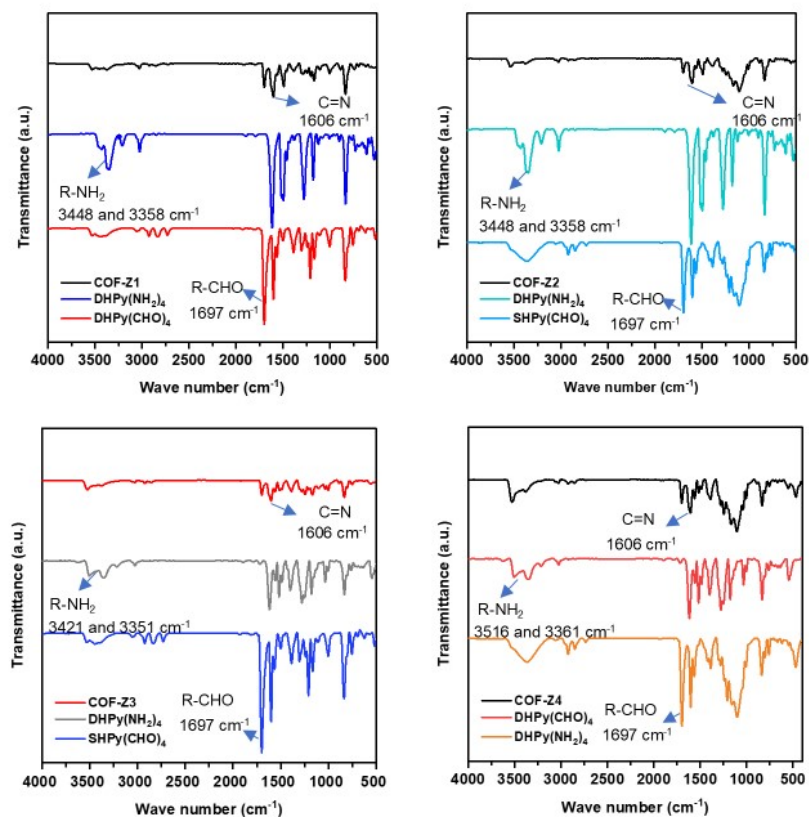


Figure S13. Fourier-transform Infrared Spectroscopy (FTIR) spectra of COF Z1, COF Z2, COF Z3 and COF Z4.

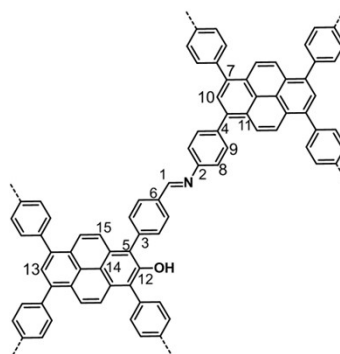
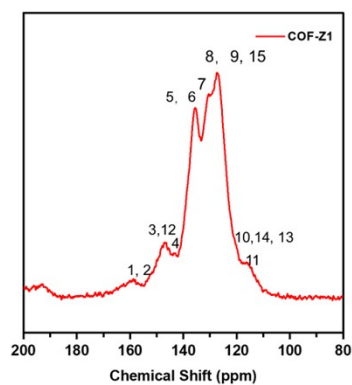


Figure S14. ^{13}C cross-polarization/magic angle spinning solid-state nuclear magnetic resonance (^{13}C CP-MAS NMR) spectrum of COF Z1.

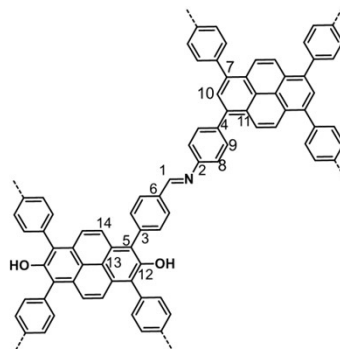
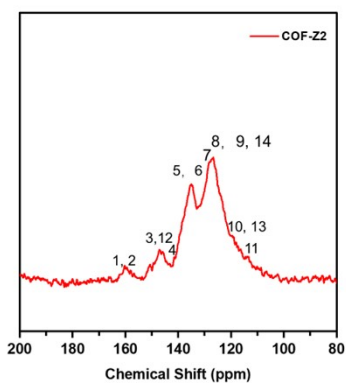


Figure S15. ^{13}C cross-polarization/magic angle spinning solid-state nuclear magnetic resonance (^{13}C CP-MAS NMR) spectrum of COF Z2.

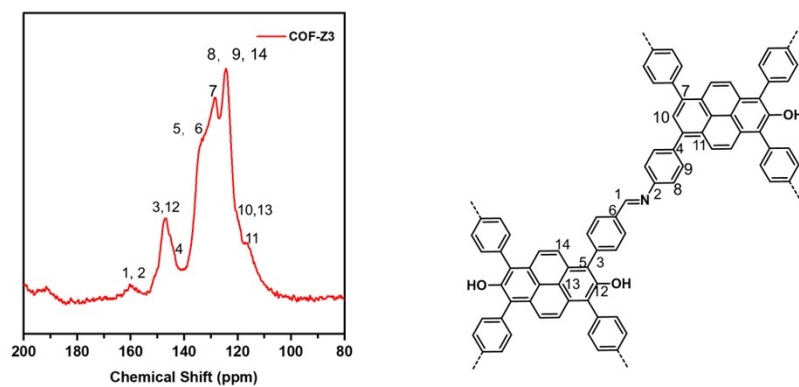


Figure S16. ^{13}C cross-polarization/magic angle spinning solid-state nuclear magnetic resonance (^{13}C CP-MAS NMR) spectrum of COF Z3.

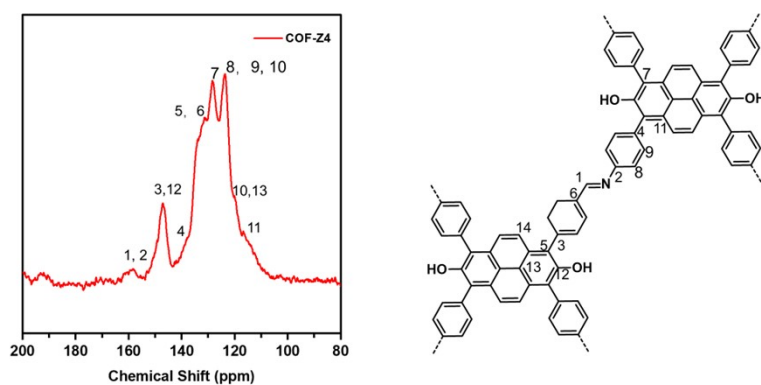


Figure S17. ^{13}C cross-polarization/magic angle spinning solid-state nuclear magnetic resonance (^{13}C CP-MAS NMR) spectrum of COF Z4.

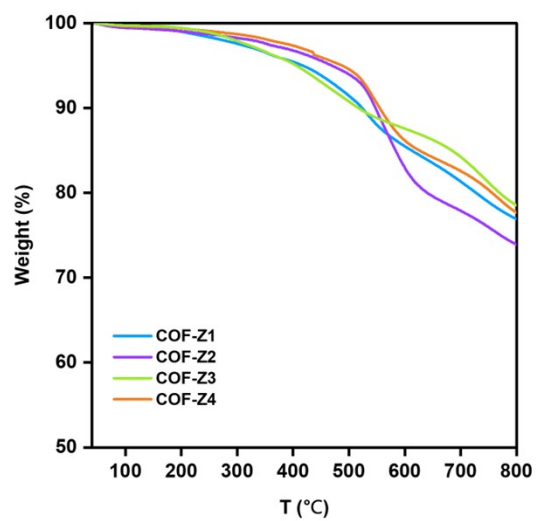


Figure S18. Thermogravimetric analysis (TGA) analysis of COF Z1, COF Z2, COF Z3 and COF Z4.

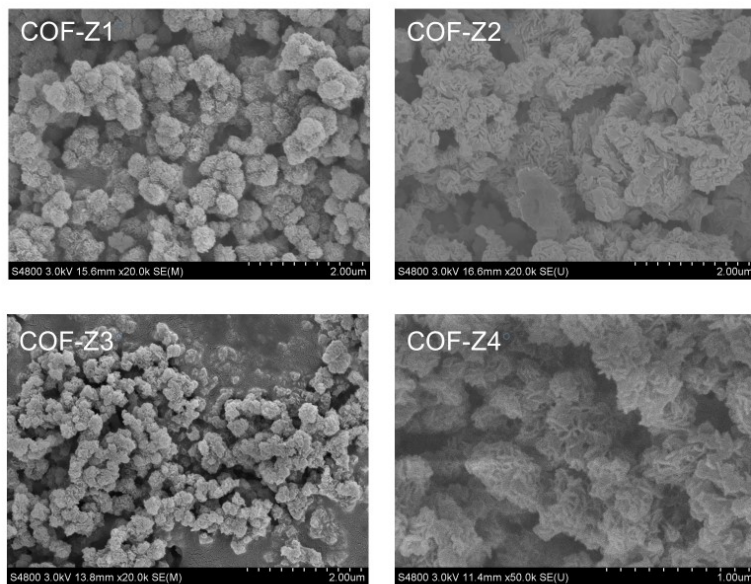


Figure S19. Scanning electron microscopy (SEM) images of COF Z1, COF Z2, COF Z3 and COF Z4.

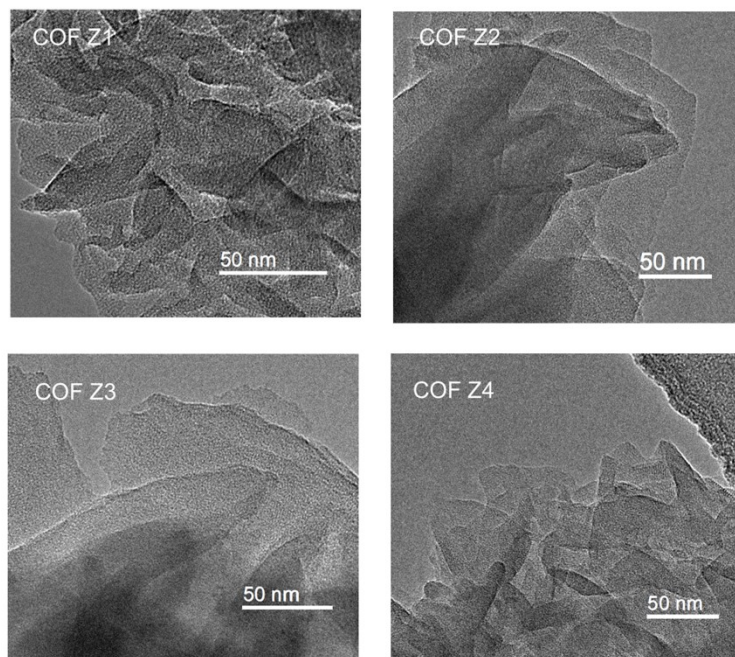


Figure S20. High-resolution transmission electron microscopy (HRTEM) images of COF Z1, COF Z2, COF Z3 and COF Z4.

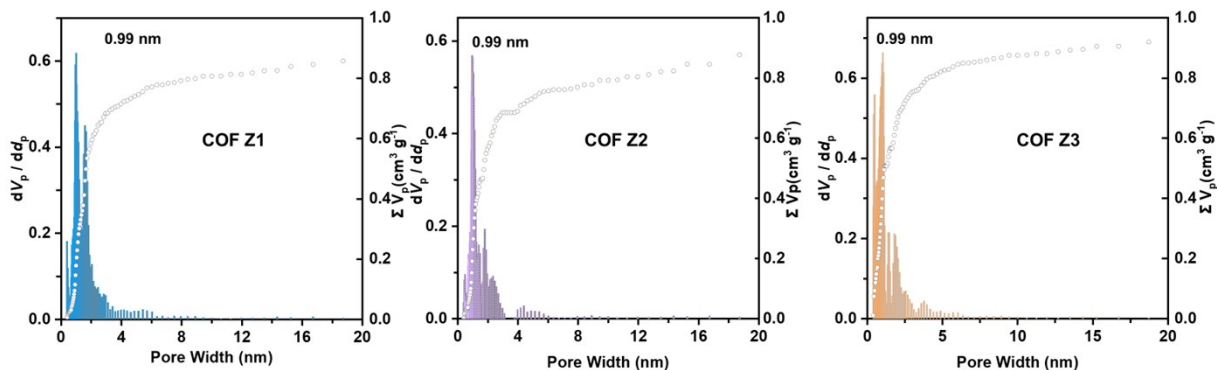


Figure S21. Pore distribution and pore volume of COF Z1, COF Z2 and COF Z3 according to nonlocal density functional theory (NLDFT) calculation.

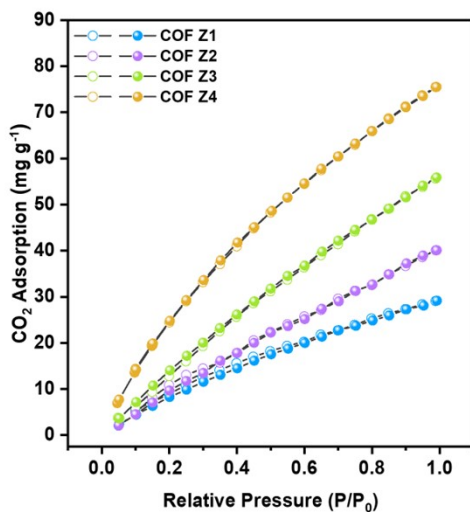


Figure S22. CO₂ adsorption isotherms of COF Z1, COF Z2, COF Z3 and COF Z4 at 298K.

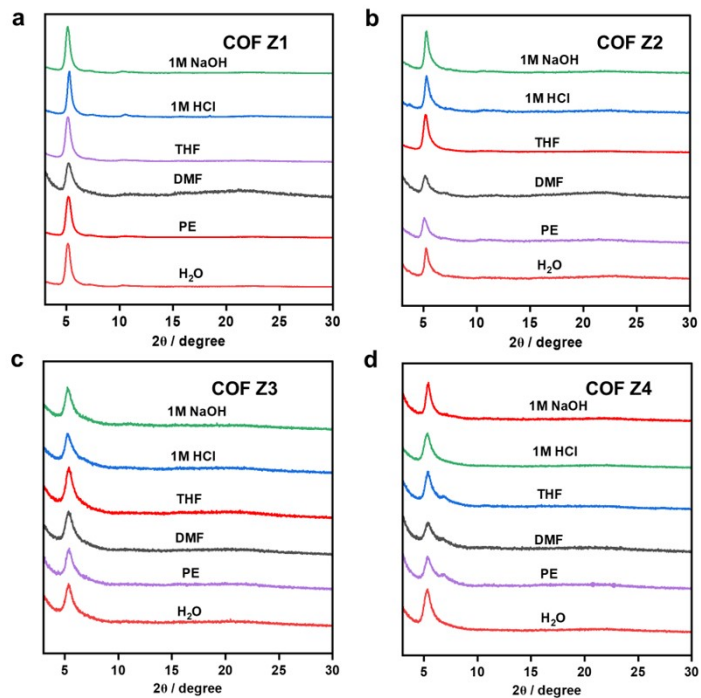


Figure S23. PXRD patterns of (a) COF Z1, (b) COF Z2, (c) COF Z3, and (d) COF Z4 after soaking under different conditions.

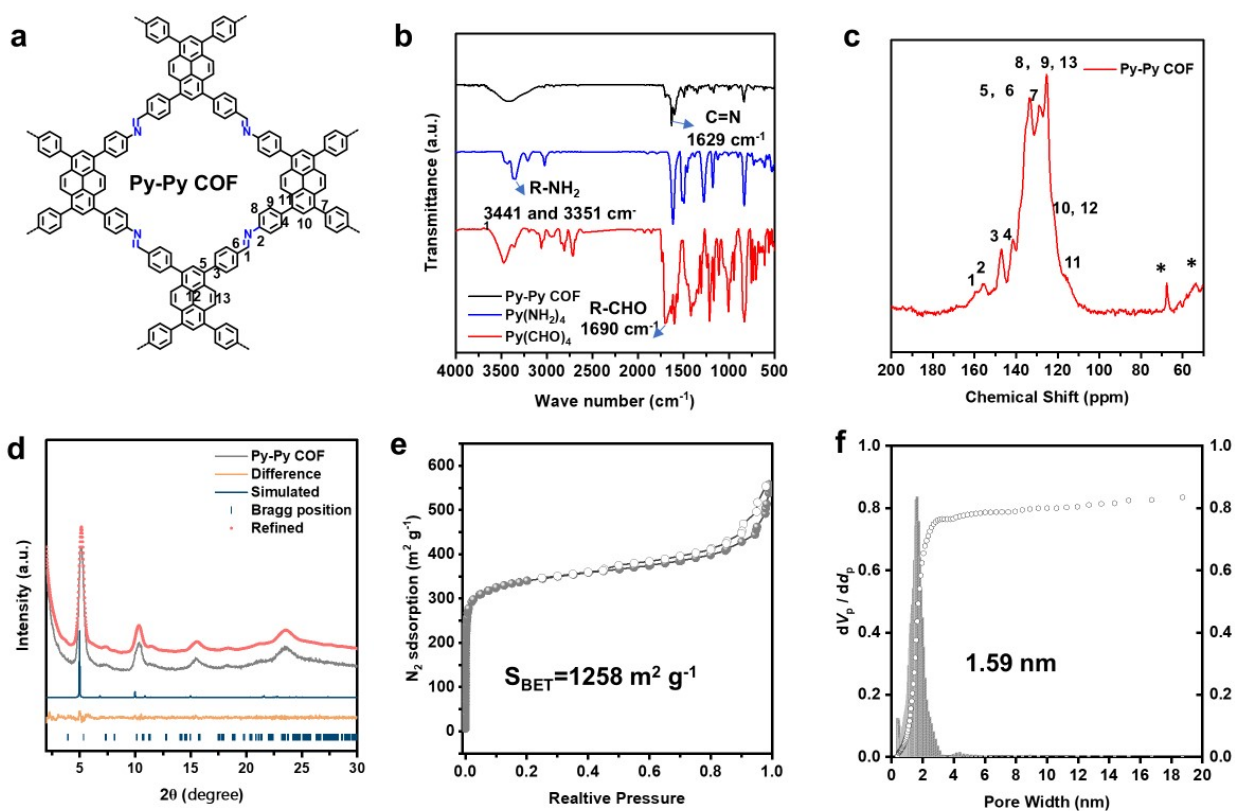


Figure S24. (a) The structure of Py-Py COF. (b) FTIR spectra of Py-Py COF. (c) ^{13}C CP-MAS NMR of Py-Py COF. (d) The PXRD pattern of Py-Py COF. (e) N_2 adsorption-desorption isotherm of Py-Py COF at 77K. (f) Pore distribution and pore volume of Py-Py COF.

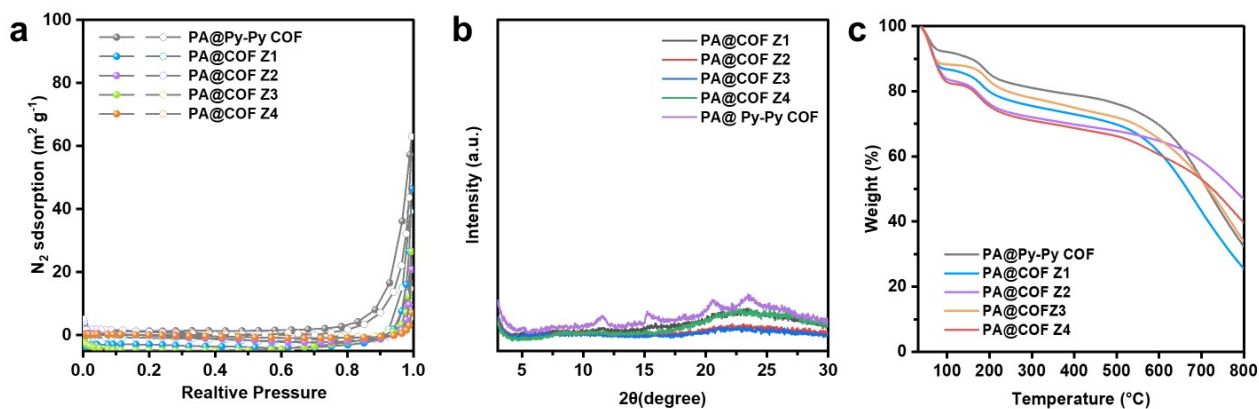


Figure S25. (a) BET surface area, (b) XRD analysis and (c) TGA analysis of PA@Py-Py COF, PA@COF Z1, PA@COF Z2, PA @ COF Z3 and PA @ COF Z4.

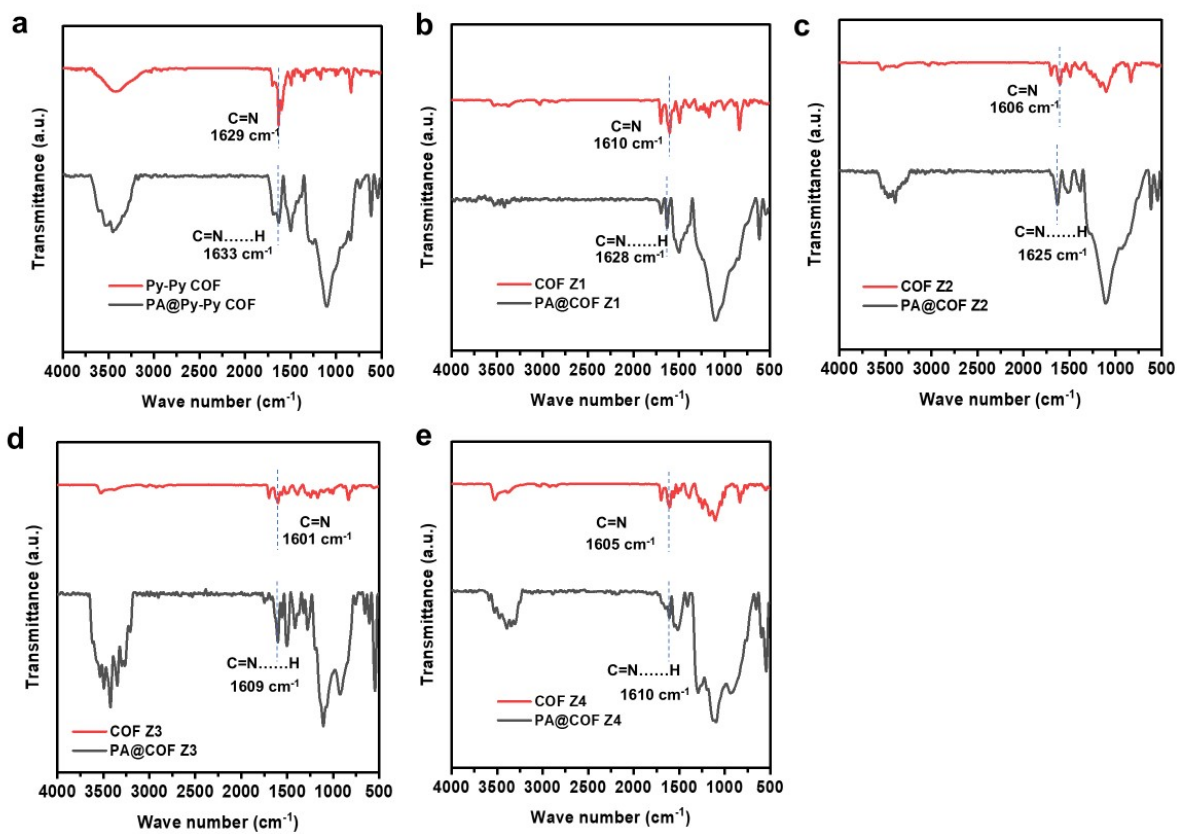


Figure S26. FTIR spectra of (a) PA@Py-Py COF, (b) PA@COF Z1, (c) PA@COF Z2, (d) PA@COF Z3, (e) PA@ COF Z4.

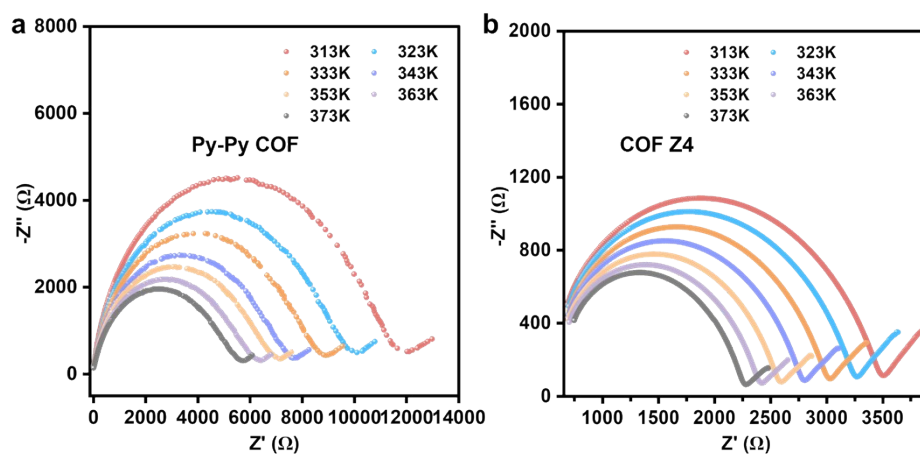


Figure S27. Nyquist plots of pristine (a) Py-Py COF and (b) COF Z4.

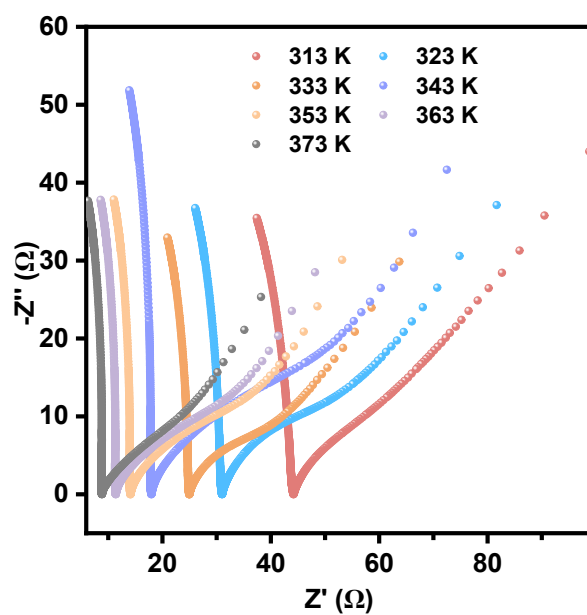


Figure S28. Nyquist plots of PA@Py-Py COF in different temperatures under R.H.=98%.

Section C. Supporting Tables

Table S1. The H₃PO₄ loading content in PA@COFs

COFs	Pore volume (cm ³ g ⁻¹)	PA@COFs	Content of H ₃ PO ₄ (wt%)
Py-Py COF	0.77	PA@Py-Py COF	140.9
COF Z1	0.87	PA@COF Z1	159.2
COF Z2	0.93	PA@COF Z2	170.2
COF Z3	0.93	PA@COF Z3	170.2
COF Z4	1.05	PA@COF Z4	192.2

Table S2. Proton conductivity values of PA@COFs

Samples	Proton conductivity under 98%R.H. (S cm ⁻¹)							E _a (eV)
	313K	323K	333K	343K	353K	363K	373K	
PA@Py-Py COF	3.24×10 ⁻³	4.61×10 ⁻³	5.79×10 ⁻³	8.05×10 ⁻³	1.02×10 ⁻²	1.26×10 ⁻²	1.62×10 ⁻²	0.13
PA@COFZ1	3.84×10 ⁻³	5.73×10 ⁻³	7.49×10 ⁻³	1.01×10 ⁻²	1.23×10 ⁻²	1.62×10 ⁻²	1.95×10 ⁻²	0.13
PA@COFZ2	3.97×10 ⁻³	5.86×10 ⁻³	7.74×10 ⁻³	1.03×10 ⁻²	1.46×10 ⁻²	1.79×10 ⁻²	2.19×10 ⁻²	0.14
PA@COFZ3	4.80×10 ⁻³	6.64×10 ⁻³	8.19×10 ⁻³	1.10×10 ⁻²	1.48×10 ⁻²	1.96×10 ⁻²	2.62×10 ⁻²	0.14
PA@COFZ4	1.40×10 ⁻²	1.92×10 ⁻²	2.59×10 ⁻²	3.32×10 ⁻²	5.01×10 ⁻²	7.36×10 ⁻²	1.09×10 ⁻¹	0.16
Samples	Proton conductivity under anhydrous conditions (S cm ⁻¹)							E _a (eV)
	373K	383K	393K	403K	413K	423K	433K	
PA@Py-Py COF	1.99×10 ⁻⁴	2.86×10 ⁻⁴	4.50×10 ⁻⁴	6.73×10 ⁻⁴	1.02×10 ⁻³	1.52×10 ⁻³	2.05×10 ⁻³	0.26
PA@COFZ1	4.31×10 ⁻⁴	6.89×10 ⁻⁴	1.05×10 ⁻³	1.54×10 ⁻³	2.35×10 ⁻³	3.26×10 ⁻³	4.52×10 ⁻³	0.25
PA@COFZ2	3.57×10 ⁻⁴	5.89×10 ⁻⁴	9.46×10 ⁻⁴	1.50×10 ⁻³	2.47×10 ⁻³	3.95×10 ⁻³	5.97×10 ⁻³	0.3
PA@COFZ3	6.43×10 ⁻⁴	9.66×10 ⁻⁴	1.43×10 ⁻³	2.08×10 ⁻³	2.90×10 ⁻³	4.15×10 ⁻³	6.00×10 ⁻³	0.24
PA@COFZ4	1.40×10 ⁻³	2.05×10 ⁻³	2.69×10 ⁻³	3.61×10 ⁻³	4.95×10 ⁻³	6.71×10 ⁻³	9.09×10 ⁻³	0.2

Table S3. List of the proton conductive materials based on COFs.

No.	Materials	σ (S cm ⁻¹)	R.H. (%)	T (°C)	E _a (eV)	References
1	<i>Nafion</i>	~1×10 ⁻¹	98	80	0.22	S1
2	H ₃ PO ₄ @NKCOF-1	1.13×10 ⁻¹	98	80	0.14	S2
3	PyBT-COF-COOH	1.5×10 ⁻²	98	80	0.41	S3
4	Aza-TT	3.4×10 ⁻²	98	95	0.25	S4
5	PA@PyTTA-BMTP-COF	7.06×10 ⁻²	90	90	-	S5
6	IPC-COF nanosheets	3.8×10 ⁻¹	98	80	0.12	S6
7	PTSA@TpAzo COFM	7.8×10 ⁻²	95	80	0.11	S7
8	COF Z4	1.09×10 ⁻¹	98	100	0.16	This work

Section D. Supporting References

- (S1) X. Wu, X. Wang, G. He and J. Benziger, *J. Polym. Sci. B: Polym. Phys.*, 2011, **49**, 1437-1445.
- (S2) Y. Yang, X. He, P. Zhang, Y. H. Andaloussi, H. Zhang, Z. Jiang, Y. Chen, S. Ma, P. Cheng and Z. Zhang, *Angew. Chem. Int. Ed.*, 2020, **59**, 3678-3684.
- (S3) S. Yang, W. Liu, Y. Zhang, X. Jia, J. Sun, C. Zhang and M. Liu, *J. Mater. Chem. A*, 2024, **12**, 28161-28169.
- (S4) Z. Li, T. Tsuneyuki, R. P. Paitandi, T. Nakazato, M. Odawara, Y. Tsutsui, T. Tanaka, Y. Miyake, H. Shinokubo, M. Takagi, T. Shimazaki, M. Tachikawa, K. Suzuki, H. Kaji, S. Ghosh and S. Seki, *J. Am. Chem. Soc.*, 2024, **146**, 23497-23507.
- (S5) S. Liu, M. Liu, X. Li, Q. Xu, Y. Sun, G. Zeng, *J. Mater. Chem. A*, 2023, **11**, 13965-13970.
- (S6) L. Cao, H. Wu, Y. Cao, C. Fan, R. Zhao, X. He, P. Yang, B. Shi, X. You, Z. Jiang, *Adv. Mater.*, 2020, **32**, e2005565.
- (S7) H. S. Sasmal, H. B. Aiyappa, S. N. Bhange, S. Karak, A. Halder, S. Kurungot, R. Banerjee, *Angew. Chem. Int. Ed.*, 2018, **57**, 10894-10898.s